

Rational Approaches to Discovery of Orally Active and Brain-Penetrable Quinazolinone Inhibitors of Poly(ADP-ribose)polymerase

Kouji Hattori,^{*,†} Yoshiyuki Kido,[†]
Hirofumi Yamamoto,[†] Junya Ishida,[†]
Kazunori Kamijo,[†] Kenji Murano,[†] Mitsuru Ohkubo,[‡]
Takayoshi Kinoshita,[‡] Akinori Iwashita,[§]
Kayoko Mihara,[§] Syunji Yamazaki,[§]
Nobuya Matsuoka,[§] Yoshinori Teramura,[#] and
Hiroshi Miyake[†]

Medicinal Chemistry Research Laboratories, Exploratory Research Laboratories, Medicinal Biology Research Laboratories, and Biopharmaceutical and Pharmacokinetic Research Laboratories, Fujisawa Pharmaceutical Co., Ltd., 2-1-6 Kashima, Yodogawa-ku, Osaka 532-8514, Japan

Received January 27, 2004

Abstract: A novel class of quinazolinone derivatives as potent poly(ADP-ribose)polymerase-1 (PARP-1) inhibitors has been discovered. Key to success was application of a rational discovery strategy involving structure-based design, combinatorial chemistry, and classical SAR for improvement of potency and bioavailability. The new inhibitors were shown to bind to the nicotinamide-ribose binding site (NI site) and the adenosine-ribose binding site (AD site) of NAD⁺.

Poly(ADP-ribose)polymerase-1 (PARP-1, EC 2.4.2.30) is a chromatin-bound nuclear enzyme involved in a variety of physiological functions related to genomic repair, including DNA replication and repair, cellular proliferation and differentiation, and apoptosis.¹ PARP-1 functions as a DNA damage sensor and signaling molecule. Upon binding to DNA breaks, activated PARP cleaves NAD⁺ into nicotinamide and ADP-ribose and polymerizes the latter into nuclear acceptor proteins including histones, transcription factors, and PARP itself. A cellular suicide mechanism of necrosis and apoptosis by PARP activation has been implicated in the pathogenesis of brain injury and neurodegenerative disorders, and PARP inhibitors have been shown to be effective in animal models of stroke, traumatic brain injury, and Parkinson's disease.^{2,3} Therefore, inhibition of PARP by pharmacological agents may be useful for the therapy of neurodegenerative disorders and several other diseases involved in PARP activation. Recently, several potent PARP inhibitors have been described using structure-based discovery; however, there remain problems in terms of the pharmacokinetics and physical properties.⁴ In this paper, we describe rational approaches to the discovery of orally active PARP inhibitors with high brain penetration.

The discovery process was initiated with a high-throughput random screening of the Fujisawa sample collection which identified **1** and **2** as seed compounds,

Table 1. Seed and Lead Profiles

	1	2	3
	PARP-1 Inhibition ^a		
IC ₅₀ (nM)	60 ± 0.12	1200 ± 60	65 ± 10
	Brain/Plasma Concentration in Mice ^b		
brain (μg/g tissue)	0.60 ± 0.035	5.5 ± 2.1	7.0 ± 1.8
plasma (μg/mL)	0.70 ± 0.16	6.7 ± 3.3	1.2 ± 0.15
ratio (B/P)	0.86	0.82	5.8

^aThe results were presented as the mean ± SE of three independent experiments. For details of assay, see Supporting Information. ^bThe results were presented as the mean ± SE. The concentration was measured at 0.5 h by HPLC after ip administration in mice at 32 mg/kg (*n* = 2).

as shown in Table 1. Quinazolinone **1** linked with large substitution exhibits strong potency against PARP-1 with an IC₅₀ of 60 nM; however, it showed poor plasma concentration after intraperitoneal administration in mice. While quinazolinone **2** exhibits an appropriately 10-fold higher plasma and brain concentration, it showed poor potency against PARP-1 (IC₅₀ = 1200 nM).⁵ We attempted to combine the desired traits of quinazolinone **2** with the potency of **1** by addition of a linked tetrahydropyridine moiety. Figure 1 conceptualizes our design proposal to find a desired lead compound based on molecular modeling of the human active site of PARP-1.⁶ Information from the previously solved X-ray structure of NAD⁺ bound to the active site of PARP-1 (Figure 1A)⁷ led us to rationally create a new inhibitor. It is strongly suggested that quinazolinone **1** and quinazolinone **2** tightly bind to the nicotinamide-ribose binding site (NI site) as a critical binding mode for a common structure motif⁸ and the 4-phenyl-tetrahydropyridine moiety of **1** provides secondary contacts to the adenosine-ribose binding site (AD site), resulting in potent IC₅₀ (Figure 1B). We designed the related quinazolinone analogue **3**, which is linked by a similar moiety extended with a three-carbon unit, by modeling to allow a maximum fit in the AD site (Figure 1C). Most of the published inhibitors bind to the NI site and/or the acceptor site but do not bind to the AD site.⁹ **1** and **3** with a unique side chain are the first inhibitors utilizing NI and AD binding sites. Lead **3** shows strong potency with an IC₅₀ of 65 nM, good bioavailability, and a significantly high brain/plasma concentration ratio (*B/P* = 6). To validate our modeling results and to improve efficiently in the new design, we performed X-ray crystallography of the catalytic domain of human PARP complexes with **1**, as shown in Figure 2.¹⁰ As expected, inhibitor **1** binds to the NI and the AD subsites of the donor site. The quinazolinone core binds to the NI site by three hydrogen bonds and by a sandwiched hydrophobic interaction with the phenyl rings of Tyr907 and Tyr896. The nitrogen atom of the tetrahydropyridine moiety directly binds to CO₂H of Asp766 located 3.6 Å from the nitrogen. The terminal phenyl ring lies in a deep pocket by van der Waals interaction. This tetrahy-

* To whom correspondence should be addressed. Phone: 81-6-6390-1220. Fax: 81-6-6304-5435. E-mail address: kouji_hattori@po.fujisawa.co.jp.

[†] Medicinal Chemistry Research Laboratories.

[‡] Exploratory Research Laboratories.

[§] Medicinal Biology Research Laboratories.

[#] Biopharmaceutical and Pharmacokinetic Research Laboratories.

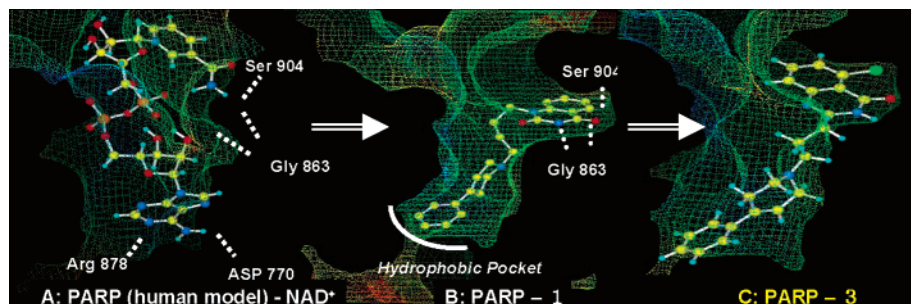


Figure 1. Molecular model of NAD⁺, **1**, and **3** in the human PARP-1 catalytic site. Accessible surface of the carbon atoms at the active sites are drawn as mesh.

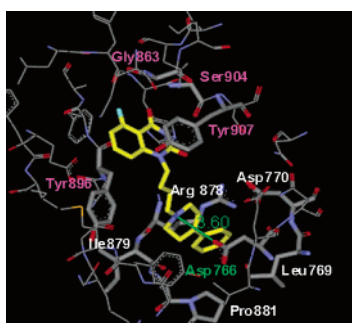
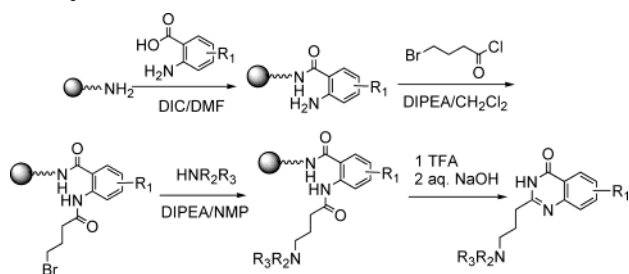


Figure 2. Compound **1** bound to the human PARP-1 active site. **1** is yellow with heteroatoms being blue for nitrogen, red for oxygen, and light-blue for fluoride. Important residues are shown stick style.

Scheme 1. Combinatorial Chemistry for Quinazolidone Library



dropyridine moiety induces a conformational change at the bottom of the AD site by motion of Arg878.¹¹

Our initial procedure to prepare quinazolinone analogues linked via appropriate substitution to establish SARs is outlined in Scheme 1. Combinatorial chemistry using solid-phase synthesis with Rink amide resin produced rapidly and efficiently the desired quinazolinone derivatives on a 10 mg scale in a total yield of 40–80%.^{12,13}

We followed basic SAR trends for three segments of the lead compound to improve the potency and bioavailability with brain penetration in the lead optimization process. Measurement of PARP inhibitory activity in vitro was carried out by a standard method using human recombinant PARP-1.¹⁴ Outlined in Table 2 are the results of several substituted derivatives of the quinazolinone core. Unsubstituted derivative **4** showed 4 times more potency than lead **3**. Improvement in activity also occurred by addition of substitution at the 6- or 8-position of the quinazolinone, while the addition of the chloro group at the 7-position (**7**) was 3 times less active than **3**. In general, addition of a chloro group to the phenyl ring improved brain concentration over **4**. The activity of 4-phenyltetrahydropyridine derivatives

Table 2. SAR of Substituted Quinazolidone Analogues

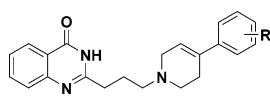
compd	R	PARP-1 IC ₅₀ (nM) ^a	brain (μg/g tissue) ^b		plasma (μg/mL) ^b	
			0.5 h	2.0 h	0.5 h	2.0 h
4	H	16	1.90	0.37	0.68	0.15
3	5-Cl	65	4.60	2.82	4.18	2.17
5	5-F	16	1.62	0.22	0.37	0.14
6	6-Cl	27	18.6	14.2	16.2	15.5
7	7-Cl	250	6.12	2.66	0.08	0.51
8	8-Cl	26	7.99	8.43	1.28	1.20
9	6,8-diCl	39	NT		NT	
10	8-Me	14	2.54	0.73	0.94	0.40
11	8-Et	66	NT		NT	
12	8-OMe	26	1.15	0.00	0.24	0.00
3-AB ^c		11200	NT		NT	

^a Values are the averages from at least two independent dose–response curves, and standard error for PARP inhibition assay is typically ±5% of the mean or less; see Supporting Information. ^b The concentration of inhibitors in brain and plasma determined in mice following po administration (32 mg/kg, *n* = 2) by ex vivo assay; see Supporting Information. ^c 3-Aminobenzamide as a standard PARP inhibitor.

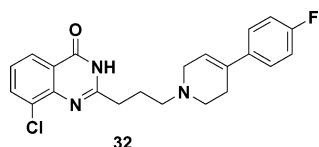
Table 3. SAR of Pyridine Analogue

Compd	R	PARP-1 IC ₅₀ (nM)	Brain(μg/g tissue)		Plasma(μg/mL)	
			0.5h	2.0h	0.5h	2.0h
4	-N-Ph	16	1.90	0.37	0.68	0.15
13	-N-Ph	46	0.37	0.10	0.25	0.00
14	-N-Ph	71	2.85	0.30	2.27	0.53
15	-C-Ph	>1000	NT		NT	
16	-N-Indole	12	NT		NT	
17	-N-Indole	74	0.58	0.15	77.2	9.51
18	-N-Phenyl	1100	NT		NT	

is outlined in Table 3. 4-Phenylpiperidine **13** and *N*-phenylpiperazine **14** had slightly less activity than **4**, while transformation from nitrogen into carbon **15** led to a complete loss of potency, suggesting that nitrogen is a key factor for binding PARP-1. The three-ring derivative **16** maintained activity, while indole derivative **17** exhibited a 100-fold higher concentration in plasma than brain. Elimination of the phenyl ring **18** showed less potency relative to the original compound. The inhibitory activity of phenyl-substituted

Table 4. SAR of Substituted Benzene Analogues


compd	R	PARP-1	brain ($\mu\text{g/g}$ tissue)	plasma ($\mu\text{g/mL}$)
		IC ₅₀ (nM)	0.5 h, 2.0 h	0.5 h, 2.0 h
4	H	16	1.90, 0.37	0.68, 0.15
19	<i>p</i> -F	8.9	3.54, 1.16	6.83, 3.48
20	<i>m</i> -F	23	NT	NT
21	<i>o</i> -F	37	NT	NT
22	<i>p</i> -Cl	23	23.9, 9.41	12.1, 2.78
23	<i>p</i> -Me	17	5.31, 2.34	5.40, 0.84
24	<i>p</i> -OH	12	NT	NT
25	<i>p</i> -OMe	8.3	5.61, 3.75	6.05, 1.67
26	<i>m</i> -OMe	1000	NT	NT
27	<i>o</i> -OMe	170	NT	NT
28	<i>p</i> -CF ₃	25	23.4, 19.5	6.80, 3.27
29	<i>p</i> -CN	6.0	4.50, 0.54	20.0, 5.20
30	<i>p</i> -Ph	34	NT	NT
31	4-Py	12	2.76, 0.30	14.1, 0.62

Table 5. Pharmacokinetics Profiles of **32**


	po (fasted), <i>n</i> = 3			iv, ^a <i>n</i> = 3		
	dose (mg/kg)	C _{max} ± SE ($\mu\text{g/mL}$)	AUC ± SE ($\mu\text{g}\cdot\text{h/mL}$)	t _{1/2} β (h)	CL _{tot} (mL/min/kg)	BA ^b (%)
mouse	10	0.30 ± 0.14	NT	NT	NT	NT
rat	10	1.33 ± 0.26	2.52 ± 0.13	1.4	13.5	20
dog	1.0	0.28 ± 0.07	3.16 ± 1.30	6.0	4.8	70

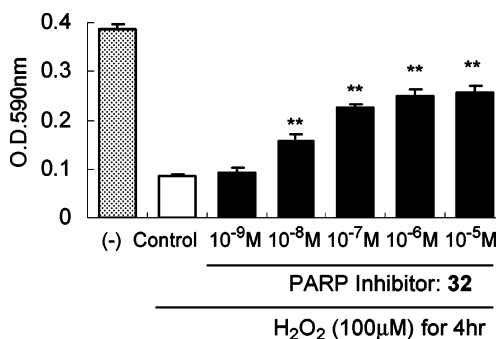
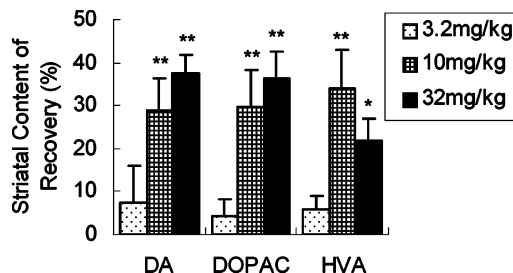
Brain/Plasma Concentration in Mice, ^c <i>n</i> = 2			
	brain ($\mu\text{g/g}$ tissue)	plasma ($\mu\text{g/mL}$)	ratio
0.5 h:	5.6 ± 2.30	1.0 ± 0.41	5.6
2.0 h:	2.1 ± 1.00	0.5 ± 0.21	4.2

Metabolism by Liver Microsomes in Vitro ^d				
	mouse	rat	dog	human
	2250 ± 104	1236 ± 69	141 ± 13	156 ± 9.5

^a Administration as the HCl salt. ^b BA = bioavailability. ^c The results were shown as the mean ± SE. The concentration was measured at 0.5 and 2.0 h by HPLC after po administration at 32 mg/kg in mice. ^d **32** was incubated at 37 °C with liver microsomes from mice, rats, dogs, and humans in the presence of the NADPH-generating system; see Supporting Information.

derivatives is outlined in Table 4. In general, substitution at the para position of the phenyl ring was more advantageous to activity than either meta or ortho substitution. A 2-fold improvement in activity was obtained by *p*-fluoro **19**, *p*-methoxy **25**, and *p*-cyano **29** with IC₅₀ = 8.9, 8.3, and 6.0 nM, respectively.

After our SAR examination and extensive research, we selected **32** as a potential candidate, since it inhibited PARP-1 activity with an IC₅₀ of 13 ± 1.1 nM (mean ± SE, *n* = 4) and was orally active with high brain penetration. Table 5 shows the pharmacokinetic profiles in mouse, rat, and dog. There was more improved bioavailability in the dog for the HCl salt of **32** (70% oral bioavailability with a 4.8 h iv half-life) than in other species, which is explained by metabolic stability as shown by measurement of in vitro clearance using liver microsomes. The concentrations of **32** in plasma and brain were measured by HPLC after oral administration

**Figure 3.** H₂O₂ induced cytoprotective effects of **32** in PC12 cells (*n* = 6): (***) *P* < 0.01.**Figure 4.** MPTP induced parkinson model of **32** in C57BL/6 mouse (*n* = 7): 100% of normal and 0% of control; (***) *P* < 0.01; (*) *P* < 0.05

in mice. Brain penetration of **32** was good with a *B/P* ratio of approximately 5.¹⁵ In addition, many recent PARP inhibitors lack good solubility in water, making them difficult to utilize in vivo. **32** and the HCl salt showed good solubility in water (260 and 5600 $\mu\text{g/mL}$, respectively).

Next, we examined the in vitro and in vivo neuroprotective action of **32**. We have already confirmed that exposure to H₂O₂ cytotoxicity induces PARP activation and poly(ADP-ribose)polymer (PAR) polymer formation in PC12 cells.¹⁶ Exposure to 150 μM H₂O₂ for 3 h produced cell damage, as evaluated by MTT assay,¹⁷ and the damage was significantly attenuated by pretreatment (1 h prior to H₂O₂ exposure) with **32** at 10⁻⁸–10⁻⁵ M in Figure 3. Figure 4 shows the effect in a mouse 1-methyl-4-phenyl-1,2,3,6-tetrahydropyridine (MPTP) model of Parkinson's disease (PD).¹⁸ The four-dose paradigm of MPTP intoxication induces severe cell injury. **32** was orally administered twice to C57BL/6 mice (3.2, 10, 32 mg/kg, po) 1 h prior to the first and third injections of MPTP, and after 4 days, each striatum was dissected to quantify dopamine (DA) and its metabolites dihydroxyphenylacetic acid (DOPAC) and homovanillic acid (HVA). In this model, pretreatment with **32** significantly prevented the depletion of striatal DA, DOPAC, and HVA contents. **32** had no monoamine oxidase-B (MAO-B) inhibitory activity and no dopamine transporter (DAT) binding affinity, suggesting that **32** was not able to affect MPTP metabolism or inhibit the accumulation of MPTP metabolites into the cells. Furthermore, **32** had no CNS toxicity in a preclinical study. Detailed pharmacological properties and the neuroprotective effects of our PARP inhibitors will be published in due course.¹⁶

We have discovered potent PARP-1 inhibitors according to a rational discovery strategy, employing random screening to find the seed, structure-based drug design by modeling to generate the lead, classical SAR and

combinatorial chemistry to optimize the lead, and X-ray analysis to validate structure conformation. The newly designed PARP-1 inhibitor **32** exhibited potent inhibitory activity in vitro and in vivo with neuroprotective activity and good bioavailability with high brain penetration. These findings suggest that **32** could be an attractive therapeutic candidate for neurodegenerative disorders such as Parkinson's disease.

Acknowledgment. We express our thanks to Dr. Kazuo Sakane and Dr. Masayuki Kato for their practical guidance and Dr. David Barrett for his critical reading of the manuscript.

Supporting Information Available: Typical experiment details and characterization for compounds **3–32**, X-ray data for **1**, and description of the in vitro PARP inhibitory assay, in vivo assay, and in vitro metabolism. This material is available free of charge via the Internet at <http://pubs.acs.org>.

References

- Recent reviews on PARP: Nguewa, P. A.; Fuertes, M. A.; Alonso, C.; Petéz, J. M. Pharmacological modulation of poly(ADP-ribose)-polymerase mediated cell death: exploitation in cancer chemotherapy. *Mol. Pharmacol.* **2003**, *64*, 1007–1014. Chiarugi, I. Poly(ADP-ribose)polymerase: killer or conspirator? The suicide hypothesis' revisited. *TIPS* **2002**, *23*, 122–129. Szabó, C.; Virag, L. The therapeutic potential of poly(ADP-ribose)polymerase inhibitors. *Pharmacol. Rev.* **2002**, *54*, 375–429. *From DNA Damage and Stress Signaling to Cell Death: Poly ADP-Ribosylation Reactions*; de Murcia, G., Shall, S., Eds; Oxford University Press: Oxford, 2000. *Cell Death: The Role of PARP*; Szabó, C., Ed.; CRC Press: Boca Raton, FL, 2000 and references therein.
- LaPlaca, M. C.; Zhang, J.; Raghupathi, R.; Li, J. H.; Smith, F.; Bareyre, F. M.; Snyder, S. H.; Graham, D. I.; McIntosh, T. K. Pharmacologic inhibition of poly(ADP-ribose)polymerase is neuroprotective following traumatic brain injury in rats. *J. Neurotrauma* **2001**, *18* (4), 369–376. Abdelkarim, G. E.; Harms, C.; Katchanov, J.; Dirnagl, U.; Szabó, C.; Endres, M. Protective effects of PJ34, a novel, potent inhibitor of poly(ADP-ribose)-polymerase (PARP) in in vitro and in vivo models of stroke. *Int. J. Mol. Med.* **2001**, *7* (3), 255–260. Takahashi, K.; Pieper, A. A.; Croul, S. E.; Zhang, J.; Snyder, S. H.; Greenberg, J. H. Post-treatment with an inhibitor of poly(ADP-ribose)polymerase attenuates cerebral damage in focal ischemia. *Brain Res.* **1999**, *829* (1–2), 46–54. Cosi, C.; Colpaert, F.; Koek, W.; Degryse, A.; Marien, M. Poly(ADP-ribose)polymerase inhibitors protect against MPTP-induced depletions of striatal dopamine and cortical noradrenaline in C57BL/6 mice. *Brain Res.* **1996**, *729*, 264–269.
- Recent studies have demonstrated that dopaminergic neurons lacking the gene coding PARP are spared from the neurotoxic effects of MPTP: Mandir, A. S.; Przedborski, S.; Jackson-Lewis, V.; Wang, Z.; Simbulan-Rosenthal, C. M.; Smulson, M. E.; Hoffman, B. E.; Guastella, D. B.; Dawson, V. L.; Dawson, T. M. Poly(ADP-ribose)polymerase activation mediates 1-methyl-4-phenyl-1,2,3,6-tetrahydropyridine(MPTP)-induced parkinsonism. *Proc. Natl. Acad. Sci. U.S.A.* **1999**, *96*, 5774–5779.
- Recent reviews: Southan, G. J.; Szabó, C. Poly(ADP-ribose)-polymerase inhibitors. *Curr. Med. Chem.* **2003**, *10*, 321–340. Cosi, C. New inhibitors of poly(ADP-ribose)polymerase and their potential therapeutic targets. *Expert Opin. Ther. Pat.* **2002**, *12*, 1047–1071.
- Some quinazolinone-based PARP inhibitors have been identified. (a) Griffin, R. J.; Srinivasan, S.; Bowman, K.; Calvert, A. H.; Curtin, N. J.; Newell, D. R.; Pemberton, L. C.; Golding, B. T. Resistance-modifying agents. 5. Synthesis and biological properties of quinazolinone inhibitors of the DNA repair enzyme poly(ADP-ribose)polymerase (PARP). *J. Med. Chem.* **1998**, *41*, 5247–5256. (b) Banasik, M.; Komura, H.; Shimoyama, M.; Ueda, K. Specific inhibitors of poly(ADP-ribose)synthetase and mono-(ADP-ribosyl)transferase. *J. Biol. Chem.* **1992**, *267*, 1569–1575.
- The human active site of PARP-1 was completely conserved with the active site of chicken of PARP-1⁷ except 763-amino acid (human, Glu763; chicken, Gln763).
- Ruf, A.; Murcia, G.; Schulz, G. E. Inhibitor and NAD⁺ binding to poly(ADP-ribose)polymerase as derived from crystal structures and homology modeling. *Biochemistry* **1998**, *37*, 3893–3900. Ruf, A.; Murcia, J. M.; Murcia, G. M.; Schulz, G. E. Structure of the catalytic fragment of poly(ADP-ribose)polymerase from chicken. *Proc. Natl. Acad. Sci. U.S.A.* **1996**, *93*, 7481–7485.
- Skalitzky, D. J.; Marakovits, J. T.; Maegley, K. A.; Ekker, A.; Yu, X.-H.; Hostomsky, Z.; Webber, S. E.; Eastman, B. W.; Almasy, R.; Li, J. Tricyclic benzimidazoles as potent poly(ADP-ribose)polymerase-1 inhibitors. *J. Med. Chem.* **2003**, *46*, 210–213. Ferraris, D.; Ficco, R. P.; Dain, D.; Ginski, M.; Lautar, S.; Lee-Wisdom, K.; Liang, S.; Lin, Q.; Lu, M. X.-C.; Morgan, L.; Thomas, B.; Williams, L. R.; Zhang, J.; Zhou, Y.; Kalish, V. J. Design and synthesis of poly(ADP-ribose)polymerase-1 (PARP-1) inhibitors. Part 4: biological evaluation of imidazobenzodiazepines as potent PARP-1 inhibitors for treatment of ischemic injuries. *Bioorg. Med. Chem.* **2003**, *11*, 3695–3707. Canan Koch, S. S.; Thoresen, L. H.; Tikhe, J. G.; Maegley, K. A.; Almasy, R. J.; Li, J.; Yu, X.-H.; Zook, S. E.; Kumpf, R. A.; Zhang, C.; Boritzki, T. J.; Mansour, R. N.; Zhang, K. E.; Ekker, A.; Calabrese, C. R.; Curtin, N. J.; Kyle, S.; Thomas, H. D.; Wang, L.-Z.; Calvert, A. H.; Golding, B. T.; Griffin, R. J.; Newell, D. R.; Webber, S.; Hostomsky, Z. Novel tricyclic poly(ADP-ribose)polymerase-1 inhibitors with potent anticancer chemopotentiating activity: design, synthesis, and X-ray cocrystal structure. *J. Med. Chem.* **2002**, *45*, 4961–4974. Costantino, G.; Macchiarulo, A.; Camaioni, E.; Pellicciari, R. Modeling of poly(ADP-ribose)polymerase (PARP) inhibitors. Docking of ligands and quantitative structure–activity relationship analysis. *J. Med. Chem.* **2001**, *44*, 3786–3794. White, A. W.; Almasy, R.; Calvert, A. H.; Curtin, N. J.; Griffin, R. J.; Hostomsky, Z.; Maegley, K.; Newell, D. R.; Srinivasan, S.; Golding, B. T. Resistance-modifying agents. 9. Synthesis and biological properties of benzimidazole inhibitors of the DNA repair enzyme poly(ADP-ribose)polymerase. *J. Med. Chem.* **2000**, *43*, 4084–4097.
- Recently, Szabó and co-workers have published new inhibitors linked to adenosine itself: Jagtap, P. G.; Southan, G. J.; Baloglu, E.; Ram, S.; Mabley, J. G.; Marton, A.; Salzman, A.; Szabo, C. The discovery and synthesis of novel adenosine substituted 2,3-dihydro-1H-isoindol-1-ones: potent inhibitors of poly(ADP-ribose)polymerase-1 (PARP-1). *Bioorg. Med. Chem. Lett.* **2004**, *14*, 81–85.
- X-ray data and the method are in the Supporting Information.
- We have also succeeded in X-ray crystallography of the catalytic domain of human PARP-1 complexes with quinazolinone derivatives. The crystal structure indicates binding to the NI site and AD subsites in a similar binding mode, as expected from modeling. The induced fitting of the inhibitors enlarges the AD site and breaks the bottom of the active site wall: Kinoshita, T.; Nakanishi, I.; Warizuka, M.; Iwashita, Y.; Kido, Y.; Hattori, K.; Fujii, T. Inhibitor-induced structural change of the active site of human poly(ADP-ribose)polymerase. *FEBS Lett.* **2004**, *556*, 43–46.
- 3** and **5** were not obtained by this method. Their resynthesis was performed using liquid synthesis and a similar method instead of using resin.
- Purity is >95% after purification, and yield is not optimized. A typical experiment method is in the Supporting Information.
- See Supporting Information.
- Measurements of the concentration of **32** in plasma and brain were performed in mice following po administration at 32 mg/kg. **32** was suspended in 0.5% methylcellulose and administered orally in a volume of 10 mL/kg. Plasma and brain were collected at 0.5 and 2 h after dosing, and the concentrations of **32** were measured using HPLC.
- Iwashita, A.; Yamazaki, S.; Mihara, K.; Hattori, K.; Yamamoto, H.; Ishida, J.; Matsuoka, N.; Mutoh, S. Neuroprotective effects of a novel poly(ADP-ribose)polymerase-1 inhibitor, 2-{3-[4-(4-chlorophenyl)-1-piperazinyl]propyl}-4(3H)-quinazolinone (FR255595), in an in vitro model of cell death and in mouse 1-methyl-4-phenyl-1,2,3,6-tetrahydropyridine model of Parkinson's disease. *J. Pharmacol. Exp. Ther.*, in press.
- Mosmann, T. Rapid colorimetric assay for cellular growth and survival: application to proliferation and cytotoxicity assays. *J. Immunol. Methods* **1983**, *65*, 55–63.
- Blum, D.; Torch, S.; Lamber, N.; Nissou, M.; Benabid, A. L.; Sadoul, R.; Verna, J. M. Molecular pathways involved in the neurotoxicity of 6-OHDA, dopamine and MPTP: contribution to the apoptotic theory in Parkinson's disease. *Prog. Neurobiol.* **2001**, *65*, 135–172. Przedborski, S.; Jackson, L. V. Mechanism of MPTP toxicity. *Movement Disord.* **1998**, *13* (Suppl. 1), 35–38. Langston, J. W. The etiology of Parkinson's disease with emphasis on the MPTP story. *Neurology* **1996**, *47*, S153–S160. Kopin, I. J.; Markey, S. P. MPTP toxicity: implications for research in Parkinson's disease. *Annu. Rev. Neurosci.* **1988**, *11*, 81–96.